REPORT DOCUMENTATION PAGE

1. REPORT DATE *(DD-MM-YYYY)*	2. REPORT TYPE	3. DATES COVERED *(From - To)*
24-06-2008	Technical Paper	

4. TITLE AND SUBTITLE	5a. CONTRACT NUMBER
Background Pressure Effects on Internal and Near-field Ion Velocity Distribution of the BHT-600 Hall Thruster (Preprint)	5b. GRANT NUMBER
	5c. PROGRAM ELEMENT NUMBER

6. AUTHOR(S)	5d. PROJECT NUMBER
Michael R. Nakles (ERC); William A. Hargus (AFRL/RZSS)	5e. TASK NUMBER
	5f. WORK UNIT NUMBER 33SP0706

7. PERFORMING ORGANIZATION NAME(S) AND ADDRESS(ES)	8. PERFORMING ORGANIZATION REPORT NUMBER
Air Force Research Laboratory (AFMC) AFRL/RZSS 1 Ara Drive Edwards AFB CA 93524-7013	AFRL-RZ-ED-TP-2008-243

9. SPONSORING / MONITORING AGENCY NAME(S) AND ADDRESS(ES)	10. SPONSOR/MONITOR'S ACRONYM(S)
Air Force Research Laboratory (AFMC) AFRL/RZS 5 Pollux Drive Edwards AFB CA 93524-7048	11. SPONSOR/MONITOR'S NUMBER(S) AFRL-RZ-ED-TP-2008-243

12. DISTRIBUTION / AVAILABILITY STATEMENT

Approved for public release; distribution unlimited (PA #08256A).

13. SUPPLEMENTARY NOTES
For presentation at the 44th AIAA Joint Propulsion Conference, Hartford, CT, 20-23 July 2008.

14. ABSTRACT

Presented is a study of the effects of chamber background pressure on the ion axial velocity distribution within the discharge chamber and in the near-field of the Busek BHT-HD-600 xenon Hall effect thruster. Ion velocity distributions were measured along the acceleration channel centerline using laser-induced fluorescence of the $5d[4]_{7/2}$-$6p[3]_{5/2}$ xenon ion excited state transition. Measurements were taken at the lowest possible chamber background pressure and a pressure that was a factor of two higher. In addition to varying the background pressure, the magnetic field of the discharge chamber was switched between two configurations. The radial magnetic was set to a low and high strength case, which produced two different anode current oscillatory regimes. Ion axial velocity distribution function peaks were used to approximate ion energy and axial electric field strength to compare the acceleration profiles of the tested thruster operating conditions. Increasing background pressure shifted the ion acceleration region upstream in the discharge chamber. The width of the velocity distributions correlated strongly to the radial magnetic field strength. The high magnetic field case data showed narrower peaks.

15. SUBJECT TERMS

16. SECURITY CLASSIFICATION OF:			17. LIMITATION OF ABSTRACT	18. NUMBER OF PAGES	19a. NAME OF RESPONSIBLE PERSON Dr. William A. Hargus, Jr.
a. REPORT Unclassified	b. ABSTRACT Unclassified	c. THIS PAGE Unclassified	SAR	10	19b. TELEPHONE NUMBER *(include area code)* N/A

Background Pressure Effects on Internal and Near-field Ion Velocity Distribution of the BHT-600 Hall Thruster   (Preprint)

Michael R. Nakles*

ERC, Inc., Edwards Air Force Base, CA 93524

William A. Hargus, Jr.†

Air Force Research Laboratory, Edwards Air Force Base, CA 93524

Presented is a study of the effects of chamber background pressure on the ion axial velocity distribution within the discharge chamber and in the near-field of the Busek BHT-HD-600 xenon Hall effect thruster. Ion velocity distributions were measured along the acceleration channel centerline using laser-induced fluorescence of the $5d[4]_{7/2} - 6p[3]_{5/2}$ xenon ion excited state transition. Measurements were taken at the lowest possible chamber background pressure and a pressure that was a factor of two higher. In addition to varying the background pressure, the magnetic field of the discharge chamber was switched between two configurations. The radial magnetic was set to a low and high strength case, which produced two different anode current oscillatory regimes. Ion axial velocity distribution function peaks were used to approximate ion energy and axial electric field strength to compare the acceleration profiles of the tested thruster operating conditions. Increasing background pressure shifted the ion acceleration region upstream in the discharge chamber changing the acceleration profile. The width of the velocity distributions correlated strongly to the radial magnetic field strength. The high magnetic field case data showed narrower peaks.

Introduction

ONe of the most significant challenges in ground testing electric propulsion devices is characterizing the effects of background chamber pressure on measured plasma properties. Alteration of the plume due to chamber effects hinders efforts to compare ground test data to numerical simulation and to predict flight characteristics of the thruster. The goal of this study was to examine the effect of background pressure on the ionization and acceleration mechanism of a low-power Hall effect thruster by measuring ion velocity distribution functions (VDF's) within the discharge chamber. Background pressure affects electron transport and thus the thruster *breathing mode*. Laser-induced fluorescence (LIF)[1] was used to experimentally measure ion velocity distribution. This technique is especially well suited for internal measurements because it is non-intrusive.

Previous internal measurements of ion velocities have been carried out using a slot cut into the side of a Hall thrusters.[2] These slots presumably affect the operation of the thruster. Even if the global effect is small, the local effect may be significant. Furthermore, slicing slots into Hall thruster side walls is not always possible with expensive, one of kind, test articles.

Most modern Hall thrusters have acceleration channels with a maximum depth of 1-2 cm. Therefore, it is possible to align collection optics to the probe beam such that limited internal optical access is possible without modification of the Hall thruster. In this work, the collection lens is placed 60° off the plume axis. This minimizes plume impact since typically greater than 95% of a Hall thruster plume ion flux is contained in a 45° half angle. In this way, it is possible to completely non-intrusively probe internal ion acceleration of any modern Hall thruster.

Experimental methods such LIF are often noise limited and are better suited to determining the most probable velocity than mean velocity. In the skewed, non-symmetric velocity distributions common to Hall thrusters, the most probable (i.e. peak signal) and statistical mean velocities often differ. Due to the

relatively narrow transition width and wide velocity distribution, these fluorescence traces have been previously shown to be representative of the ion velocity distribution function VDF.[3]

Acceleration channel centerline ion velocities were measured for two different chamber background pressures. Measurements were taken at the lowest possible chamber background pressure and a pressure that was a factor of two higher. In addition to varying the background pressure, the magnetic field of the discharge chamber was switched between two configurations. The radial magnetic was set to a low and high strength case; the high strength case being a factor of two higher in magnitude. Changing the magnetic field altered the discharge current oscillation magnitude. The goal of this study is to characterize the effects on the ion acceleration profile produced by varying background pressure and magnetic field.

Experimental Apparatus

Xenon Ion Spectroscopy

LIF is a convenient diagnostic for the investigation of ion and atomic velocities as it does not perturb the plasma. The LIF signal is a convolution of the VDF, transition line shape, and laser beam frequency profile. Determination of the VDF from LIF data only requires the deconvolution of the transition line shape and laser beam profile from the raw LIF signal trace.

For the results reported here, the $5d[4]_{7/2} - 6p[3]_{5/2}$ electronic transition of Xe II at 834.7 nm is probed. The isotopic and nuclear-spin effects contributing to the hyperfine structure of the $5d[4]_{7/2} - 6p[3]_{5/2}$ xenon ion transition produce a total of 19 isotopic and spin split components. The hyperfine splitting constants which characterize the variations in state energies are only known for a limited set of energy levels. Unfortunately, the 834.7 nm xenon ion transition only has confirmed data on the nuclear spin splitting constants of the $6p[3]_{5/2}$ upper state.[2, 4–6] Manzella first used the $5d[4]_{7/2} - 6p[3]_{5/2}$ xenon ion transition at 834.7 nm to make velocity measurements in a Hall thruster plume.[7] A convenient feature of this transition is the presence of a relatively strong line originating from the same upper state ($6s[2]_{3/2} - 6p[3]_{5/2}$ transition at 541.9 nm,[8] which allows for non-resonant fluorescence collection). Ion velocity is simply determined by measurement of the Doppler shift of the absorbing ions.[9]

Previous measurements and analysis have shown that deconvolution is not strictly required to estimate xenon ion VDFs from the raw LIF data in this plasma discharge for this particular xenon transition.[3] The transition is relatively narrow (approximately 600 MHz) and the VDF in the vicinity of the exit plane is sufficiently broad that the fluorescence trace does not require deconvolution of the transition line shape to produce an adequate estimate of the VDF. Not performing the deconvolution further in the plume (e.g. beyond the cathode plane) may introduce uncertainties estimated to be less than 20%. Zeeman splitting is neglected in this analysis due to the broad velocity distributions.

Test Facility

The LIF measurements were performed in Chamber 6 of the Air Force Research Laboratory (AFRL) Electric Propulsion Laboratory at Edwards AFB, CA. Chamber 6 is a non-magnetic stainless steel chamber with a 1.8 m diameter and 3 m length. It has a measured pumping speed of 32,000 l/s on xenon. Pumping is provided by four single stage cryogenic panels (single stage cold heads at 25 K) and one 50 cm two stage cryogenic pump (12 K). Chamber pressure during nominal thruster operation is approximately 1.5×10^{-5} Torr, corrected for xenon.

The thruster is mounted on a three axis orthogonal computer controlled translation system. Figure 1 shows the Hall thruster and optics mounted within the vacuum chamber as well as the LIF apparatus. The laser is a tunable diode laser. It is capable of tuning approximately ± 50 GHz about a center wavelength of 834.7 nm. The 6 mW beam is passed through a Faraday isolator to eliminate feedback to the laser. The laser beam then passes through several beam pick-offs until it is focused by a lens and enters the vacuum chamber through a window. The probe beam is chopped at a frequency by an optical chopper (Ch2 at 2.8 kHz) for phase sensitive detection of the fluorescence signal.

The two wedge beam pick-offs (BS) shown in Fig. 1 provide portions of the beam for diagnostic purposes. The first beam pick-off directs a beam to a photodiode detector (D1) used to provide constant power feedback to the laser. The second beam is divided into two equal components by a 50-50 cube beam splitter. The first component is directed to a Burleigh WA-1500 wavemeter used to monitor absolute wavelength. The second component is sent through an optical chopper (Ch1 at 1.4 kHz) and through a low pressure xenon hollow cathode discharge lamp. The lamp provides a stationary absorption reference for the determination of the Doppler shift. Unfortunately, there is no detectable population of the ionic xenon $5d[4]_{7/2}$ state. However, there is a nearby (estimated to be 18.1 GHz distant) neutral xenon $6s'[1/2]_1 - 6p'[3/2]_2$ transition at 834.68 nm.[10, 11] The second pick-off sends a beam to a 300 MHz free spectral range Fabry-Perot etalon (F-P) that provides
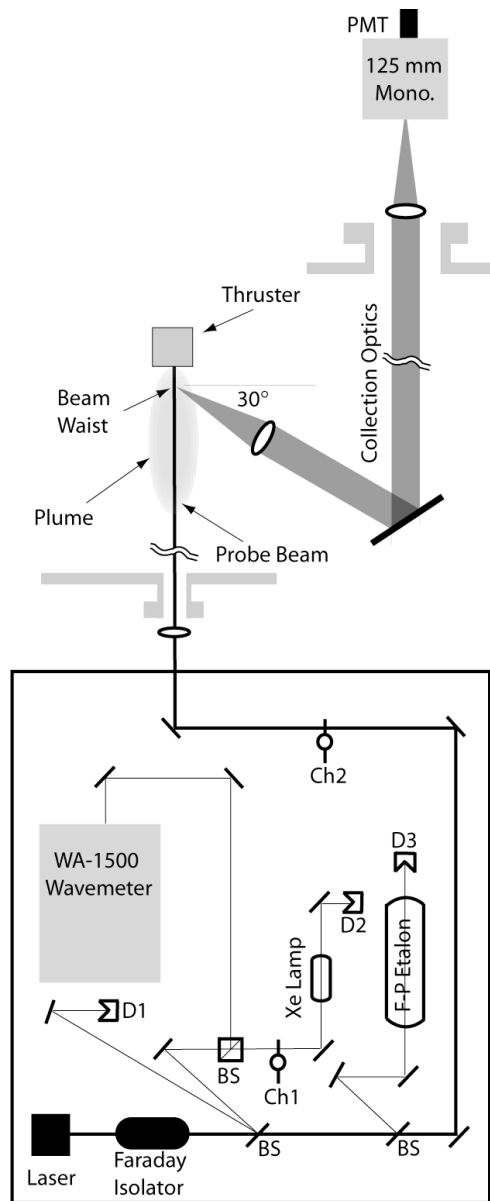
Figure 1. Diagram of the laser optical train and collection optics.

Figure 2. Photograph of the Busek BHT-HD-600 Hall effect thruster.

high resolution frequency monitoring of the wavelength interval swept during a laser scan.

The fluorescence collection optics are also shown in Fig. 1. The fluorescence is collected by a 75 mm diameter, 300 mm focal length lens within the chamber and oriented 60° from the probe beam axis. The collimated fluorescence signal is directed through a window in the chamber side wall to a similar lens that focuses the collected fluorescence onto the entrance slit of 125 mm focal length monochrometer with a photomultiplier tube (PMT). Due to the 1:1 magnification of the collection optics, the spatial resolution of the measurements is determined by the geometry
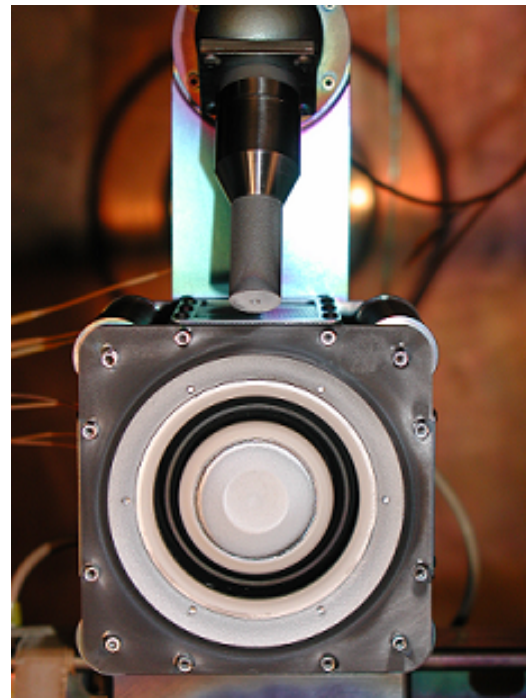
of the entrance slit 0.7 mm width and 1.5 mm height as well as the sub-mm diameter of the probe beam. This apparatus allows for limited probing of the interior acceleration channel of Hall thrusters with relatively shallow acceleration channels. Measurements show that this combination of apparatus and laser power are well within the linear fluorescence regime.

Hall Effect Thruster

The Hall thruster used in this study is the rectangular 600 W Busek Company BHT-HD-600 Hall thruster with a Busek 3.2 mm hollow cathode. A photograph of the rectangular BHT-HD-600 Hall thruster is shown in Fig. 2. This thruster has a conventional five magnetic core (one inner, five outer) magnetic circuit. The acceleration channel of the thruster has a 32 mm outer radius and a 24 mm inner radius. The acceleration channel has a depth of approximately 10 mm between the geometrical exit plane and the furtherest forward extent of the anode. The thruster has been extensively characterized to have a thrust of 39 mN with a specific impulse of 1,530 s yielding an efficiency of approximately 50% at the nominal conditions specified in Table 1.

Figure 3 shows a cut-a-way view of the near field geometry of the Busek BHT-600 Hall thruster. The locations of the central magnetic poles and edges of the acceleration channel are indicated as is the position of the cathode. The Cartesian coordinate system
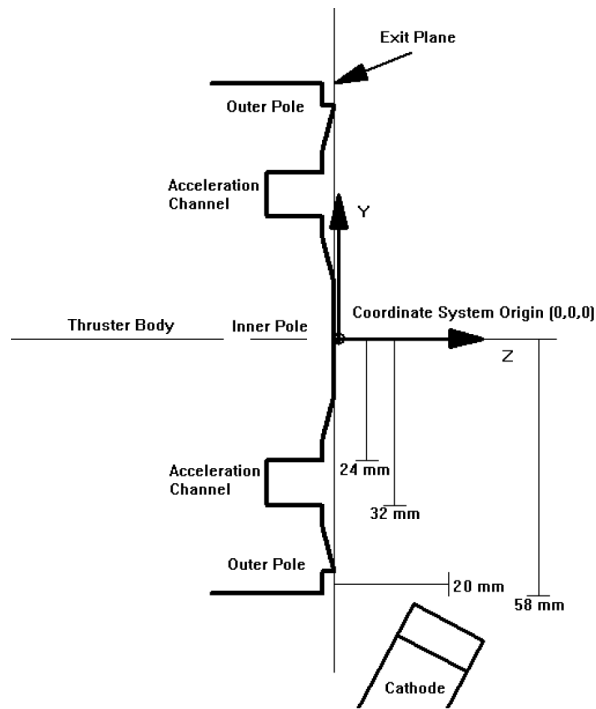
Figure 3. Cross-section of the BHT-HD-600 Hall thruster showing coordinate system of LIF measurements.

and origin used in these measurements are also shown in Fig. 3 , with positive x axis going into the page. The origin is at the center of the thruster face due to the ease and repeatability with which this position could be located. All measurements presented in this work will lie on the $z = 0$ mm and $z = +28$ mm line. This corresponds to the acceleration channel centerline.

Results and Discussion

Pressure and Magnetic Field Variations

The measured background pressure in Chamber 6 was 1.5×10^{-5} Torr (corrected for xenon) during nominal testing of the BHT-HD-600. Chamber pressure was

Table 1. Nominal BHT-HD-600 Hall thruster operating conditions.

Anode Flow	2.453 mg/s
Cathode Flow	197 μg/s
Anode Potential	300 V
Anode Current	2.16 A
Keeper Current	0.5 A
Heater Current	3.0 A

measured using a cold cathode gauge. Data was taken at this pressure for a representative *low pressure* case. In order to increase the background pressure for this study, extra Xe gas was flowed into the chamber. For the *high pressure* case, an extra 27.5 sccm was fed into the chamber behind the thruster, doubling the background pressure to 3.0×10^{-5} Torr.

Varying the magnetic field by changing the applied current to either of the four series connected outer magnetic cores, and/or the central core allowed for the examination of two distinct anode current oscillatory conditions. The two oscillatory conditions were studied at each background pressure condition. The *high magnetic field* configuration had twice the radial magnetic field strength as the *low magnetic field* case. Despite the change in field strength, the shape of the radial field profile remained similar. Figure 4 shows the normalized radial field profiles along the acceleration channel centerline calculated using the Maxwell software simulation package.
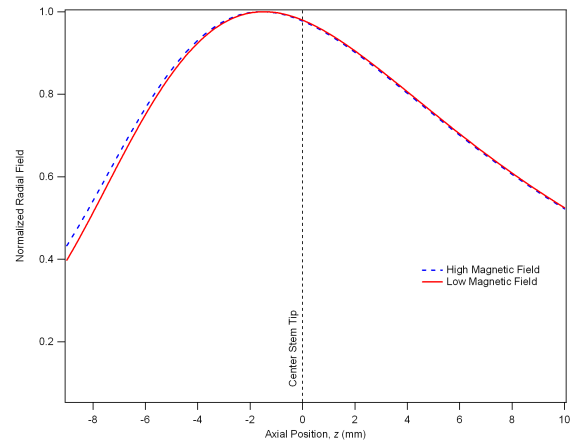

Figure 4. Normalized radial magnetic field strength along the acceleration channel centerline. The radial field strength is a factor of two greater in the high case than in the low case. However, the profile of the radial field strength is nearly identical in both cases.

Anode Current Oscillations

The variation of magnetic field strength resulted in two distinct anode current oscillatory regimes. Figure 5 displays the anode current fluctuations with time along with the corresponding frequency spectrum. The high magnetic field case produced a mode where the oscillations were small relative to the mean current. The oscillations appear to be broadly spread between 10 and 100 kHz. A more dynamic mode appeared for the low magnetic field case where the amplitude of the anode current oscillations was large. This mode exhibited a strong peak frequency of 44 kHz which in the time domain plots is seen as

a more coherent sinusoid oscillation that dominated the anode current. The low magnetic field case also differed by displaying a significant second harmonic frequency. Despite the varying oscillation patterns, the mean current was similar among the four different combinations of magnetic field and background pressure (only varying by a few percent). These oscillatory modes appear to be consistent with the *breathing mode oscillation* that has been seen by others.[12] The breathing mode oscillation can be characterized as axial instability that produces an instability in the region of ionization as well as local plasma potentials. A more detailed analysis of the effect of current oscillations on ion velocity distributions can be found in Ref. 13.

Magnetic field strength was the main factor in the oscillatory behavior of the anode current, however background pressure variation also made measurable contributions. In the high magnetic field case, high chamber pressure was observed to increase the magnitude of the anode current oscillations. The standard deviation of the current went up by 44%. The peak oscillation frequency also increased from 43.1 to 44.5 kHz. The effect of higher chamber pressure was less pronounced for the low magnetic field. Here the standard deviation of the current only increased by 12%. However, the frequency spectrum displayed an increase in the presense of high frequency oscillations near the second harmonic.
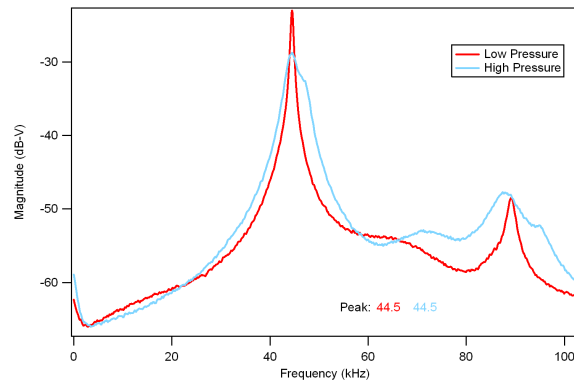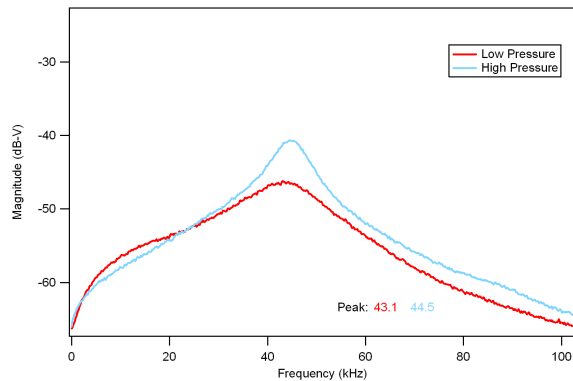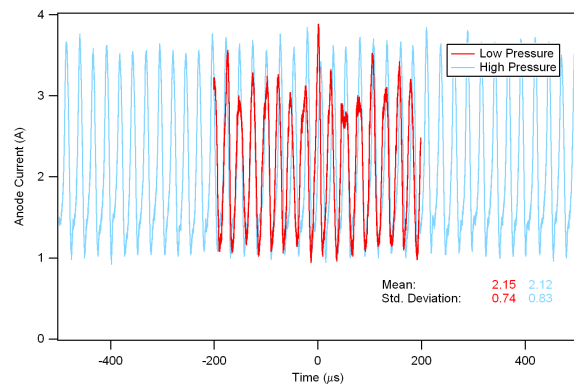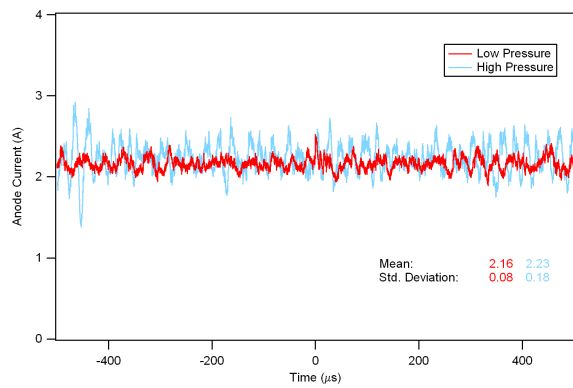
Ion Velocity Distribution

Ion velocity distribution functions were measured along the along the centerline of the acceleration channel ($y = 28$ mm) from just downstream of the anode (z=-9 mm) to 10 mm downstream of the center stem tip (z=10 mm). The measurements were taken in the $x - y$ plane ($x = 0$).

Figure 6 displays the trend of the VDF's throughout the acceleration region for all four cases. At low background pressure, the introduction of strong anode current oscillations produces much broader velocity distributions. Presumably due to the oscillations in the local anode potential that occurs during the relatively long LIF integration times, typically 4-7 minutes. The effect is dramatic. The velocity distributions of the low magnetic field strength case are very broad and appear to indicate that the local plasma potential is dithering between ionization (at near zero velocity) and significantly higher acceleration than the high magnetic field case. The final effect is that the anode current oscillations appear to result in significantly broader velocity distributions.

The effect of increasing the pressure by a factor of two is very different than the introduction of anode oscillations. In both oscillatory cases, the acceleration is pushed significantly downstream by the raising of the chamber background pressure. In the high magnetic field strength, low oscillation case, there is also a perceptible broadening of the velocity distribution. This broadening is more prevalent in the deep interior and less prominent downstream. Interestingly, the peak and mean velocities appear to be higher for the high pressure cases, perhaps indicating that the high pressure cases are more efficient at recovering the applied discharge potential. The effect of increasing the vacuum chamber background pressure in the low magnetic strength, highly oscillatory case is similar in the deep interior in that the velocity distributions are broadened. However beyond the exit plane, the high background pressure cases are actually less broadened than the low pressure case. This may be indicative of interactions with the background neutrals or signal other changes in the behavior of the ion velocity distribution.
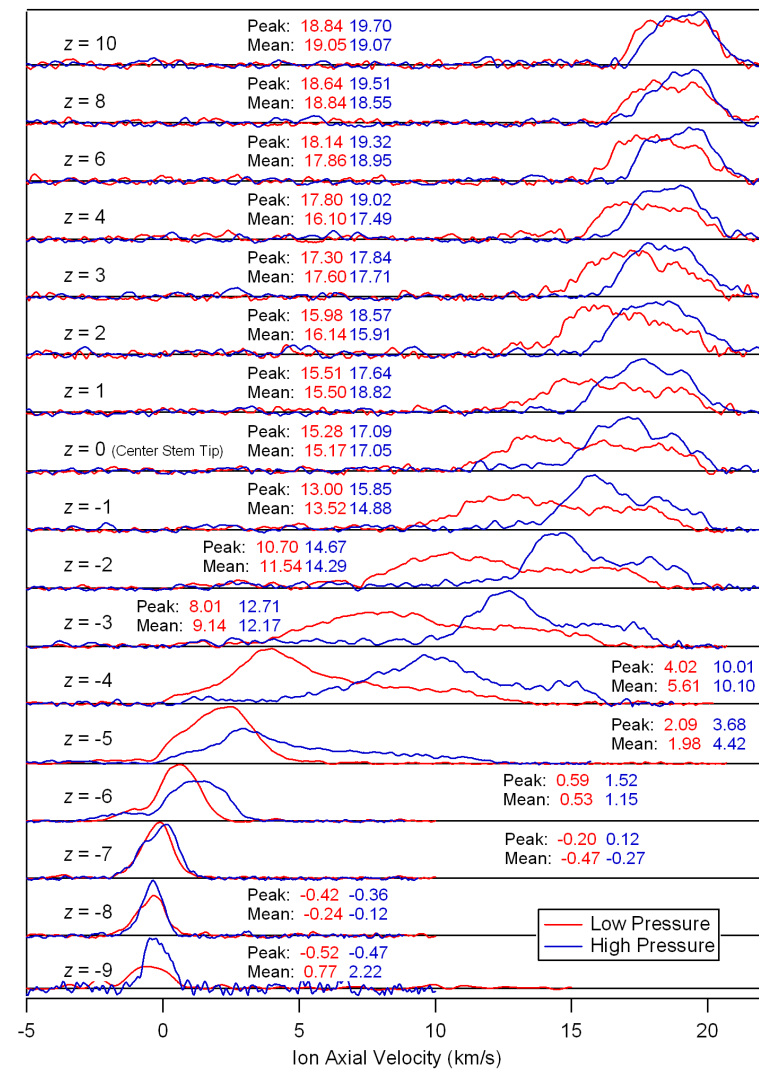
(a) High Magnetic Field Case

(b) Low Magnetic Field Case

Figure 5. Anode current time and frequency domain behavior.
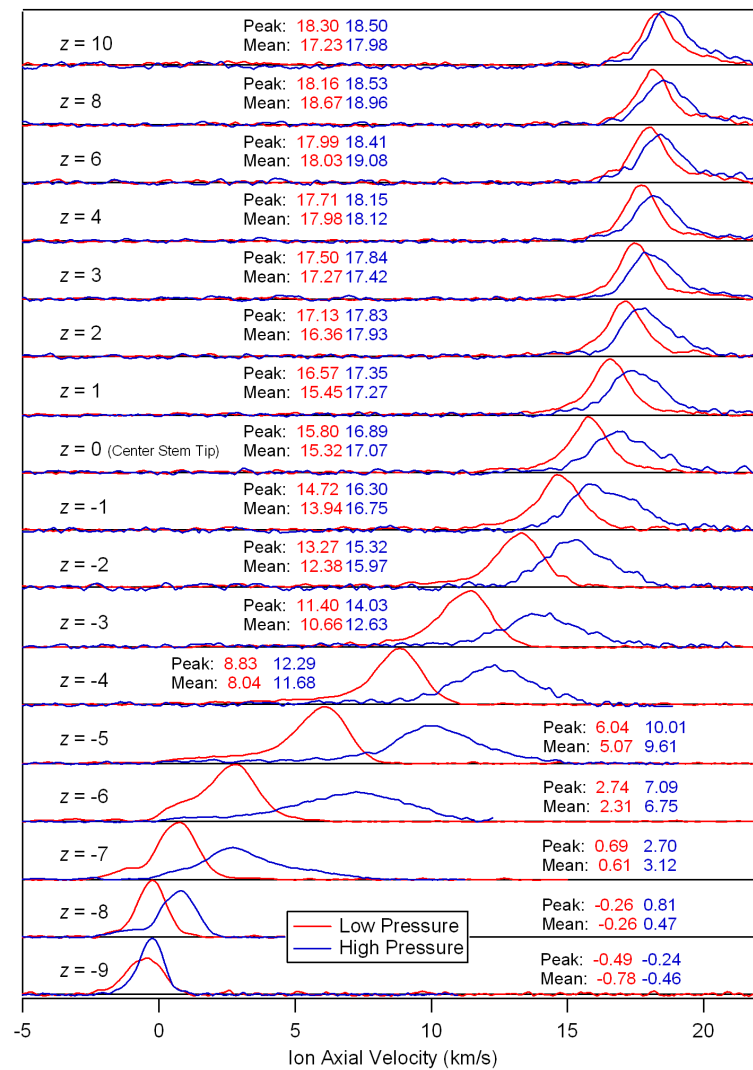
(a) High Magnetic Field Case

(b) Low Magnetic Field Case

Figure 6. Axial ion velocity distribution functions along the acceleration channel centerline. Units: Axial position, z: mm, Peak and Mean Velocity: km/s. Peaks are area normalized to unity.

From Fig. 7, it is apparent that the low oscillation, high magnetic field strength case electric field is shifted almost 2 mm downstream, but retains much of its basic shape. The reason for this shift downstream is not precisely known, but has been observed previously when propellant flow rates were increased.[14] This shift in the electric field may be due to greater neutral ingestion which provides a greater density of electron collision partners. A greater collision frequency would raise the classical electron conductivity and perhaps push the electric field further into the acceleration channel. The increased width of the ion velocity distribution with increased pressure may be due to increased overlap between the ionization and acceleration portions of the ion flow within the acceleration channel. Although the increases in the magnitude of the oscillations may also be responsible if it produces axial variations in the accelerating potential.

In contrast, the high oscillation, low magnetic field case has a higher electric field at low background pressure than the low oscillation, high magnetic field case, but only by approximately 10%. The peak of the electric field is moved downstream and resides in the region of maximum VDF width between $z = -4$ mm and the thruster exit plane. This is consistent with the supposition that the increased oscillations cause increased electron transport due to plasma turbulence, in this case in the form of axial oscillations. However when the background pressure is increased, the electric field of the high oscillation, low magnetic field case is significantly changed in magnitude and shape. The increase in background pressure produces profound differences in the electric field profile of the high oscillation, low magnetic field case. The peak electric field shifts upstream nearly 3 mm and peak electric field increases by over 30%. This modest increase in background pressure ($2\times$) has a tremendous effect on the ion acceleration within the Hall effect thruster, and this effect is most pronounced when there are axial disturbances within the discharge.

One note of caution should be sounded in this analysis of the electric fields. The fields shown in Fig. 7 are not only calculated using the most probable velocity to calculate the most probable ion energy, but by their very nature are time averaged. It appears that the plasma potential within the acceleration channel is in fact oscillating at high frequencies and the instantaneous electric field is in fact radically different than the time average that we are deriving from the LIF measurements. There is value in the time averaged quantity in this from the perspective of studying thruster erosion, predicting lifetime, and assessing thruster performance. However, it must be remembered that these LIF data cannot be used to study instantaneous plume properties.

Summary and Conclusions

This study examined the effects of chamber background pressure on the ion axial velocity distribution within the discharge chamber and in the near-field of a medium power Hall thruster. The measured ion velocity distributions in the center of the acceleration channel centerline were taken at two background pressures which differed by a factor of two. In addition to varying the background pressure, the thruster magnetic field strength was also varied by a factor of 2. This produced two different anode current oscillatory regimes. Ion axial velocity distribution function peaks were used to approximate ion energy and axial electric field strength to compare the acceleration profiles of the tested thruster operating conditions. Increased discharge oscillations had the effect of increasing the VDF, particularly within the acceleration channel. Increasing background pressure shifted the ion acceleration region upstream, while increasing the discharge oscillations increased the peak electric field and shifted it downstream toward the exit plane. The effect both increasing the oscillations and the background pressure produced profound changes in the shape of the electric field and its peak location. To some extent the two effects actually counteracted one another.

The strongest effect of the increased oscillations to significantly broaden the VDF. This is likely an indication of the oscillation of the thruster breathing mode which produces a dithering of the local plasma potential and thus affects the local instantaneous ion velocities. Increasing the background pressure seems to increase this effect within the thruster, but also damps this effect in the near plume.

Interestingly, the peak ion velocity (and hence energy) is higher for the more oscillatory cases. This includes the oscillations induced by raising the background pressure. The extent of any performance gain or loss has not yet been characterized. However, it is interesting to note the introduction of oscillations moves the time averaged peak electric field downstream and increases the peak value. It is not yet known what the trade off is with respect to lifetime between moving the peak electric field downstream and producing higher energy ions deep within the acceleration channel due to the oscillations in the local plasma potential.

Background pressure effects on thruster operation appear to be a complex issue and are not a simple addition to the discharge current due to ingestion. The effect of background pressure changes the acceleration profile and the oscillatory behavior of the

(a) High Magnetic Field Case
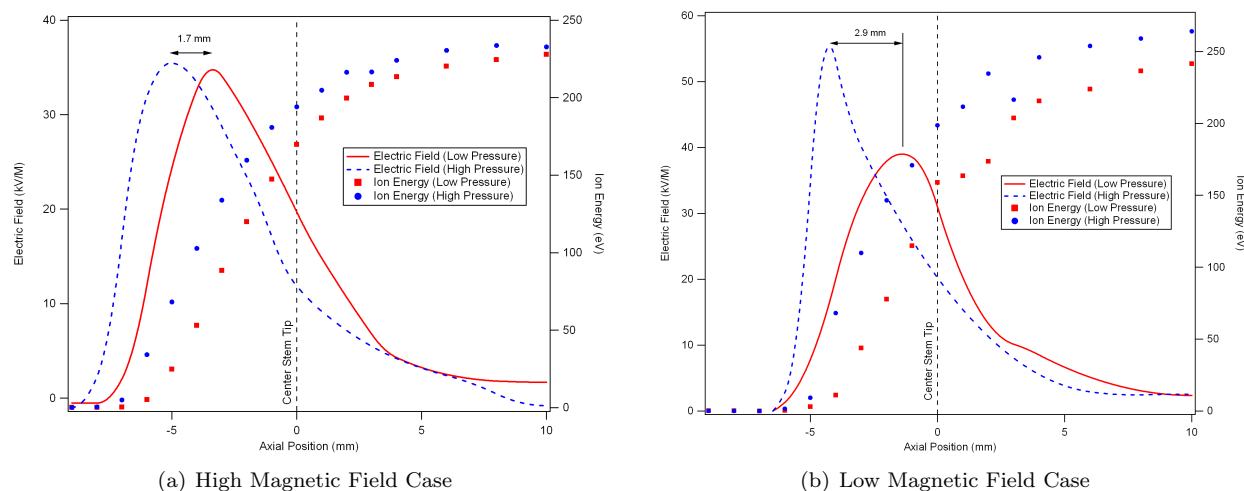

(b) Low Magnetic Field Case

Figure 7. Ion energy distribution peak profile and derived axial electric field strength. Electric field strength was approximated by differentiating ion energy peak with respect to z. (Note: Ion energy peak function was smoothed before differentiation.)

thruster. This has serious implications for the understanding of ground based testing of Hall thrusters. Randolph et al.[15] have previously proposed that operation of Hall thrusters below 5×10^{-5} Torr is sufficient to minimize the background pressure effects. The measurements in this work show that the effect of varying pressures below 5×10^{-5} Torr remains a serious issue and requires further investigation.

Acknowledgments

References

[1]Hargus, Jr., W. A., *Investigation of the Plasma Acceleration Mechanism Within a Coaxial Hall Thruster*, Ph.D. thesis, Stanford University, Stanford, CA, 2001.

[2]Hargus Jr., W. A. and Cappelli, M. A., "Laser-Induced Fluorescence Measurements of Velocity within a Hall Discharge," *Applied Physics B*, Vol. 72, No. 8, June 2001, pp. 961–969.

[3]Hargus Jr., W. A. and Nakles, M. R., "Evolution of the Ion Velocity Distribution in the Near Field of the BHT-200-X3 Hall Thruster," *Proceedings of the 42nd Joint Propulsion Conference and Exhibit*, No. AIAA-2006-4991, American Institute of Aeronautics and Astronautics, July 2006.

[4]Geisen, H., Krumpelmann, T., Neuschafer, D., and Ottinger, C., "Hyperfine Splitting Measurements on the 6265 Angstrom and 6507 Angstrom Lines of Seven Xe Isotopes by LIF on a Beam of Metastable Xe(3P0,3) Atoms," *Physics Letters A*, Vol. 130, No. 4-5, July 1988, pp. 299–309.

[5]Fischer, W., Huhnermann, H., Kromer, G., and Schafer, H. J., "Isotope Shifts in the Atomic Spectrum of Xenon and Nuclear Deformation Effects," *Z. Physik*, Vol. 270, No. 2, January 1974, pp. 113–120.

[6]Bronstrom, L., Kastberg, A., Lidberg, J., and Mannervik, S., "Hyperfine-structure Measurements in Xe II," *Physical Review A*, Vol. 53, No. 1, January 1996, pp. 109–112.

[7]Manzella, D. H., "Stationary Plasma Thruster Ion Velocity Distribution," *Proceedings of the 30th Joint Propulsion Conference and Exhibit*, No. AIAA-1994-3141, American Institute of Aeronautics and Astronautics, June 1994.

[8]Hansen, J. E. and Persson, W., "Revised Analysis of Singly Ionized Xenon, Xe II," *Physica Scripta*, , No. 4, 1987, pp. 602–643.

[9]Demtroder, W., *Laser Spectroscopy: Basic Concepts and Instrumentation*, Springer-Verlag, 1996.

[10]Miller, M. H. and Roig, R. A., "Transition Probabilities of Xe I and Xe II," *Physical Review A*, Vol. 8, No. 1, July 1973, pp. 480–486.

[11]Moore, C. E., *Atomic Energy Levels*, Vol. II, National Bureau of Standards, 1958.

[12]Choueiri, E., "Plasma Oscillations in Hall Thrusters," *Physics of Plasmas*, Vol. 8, No. 4, April 2001, pp. 1411–1426.

[13]Hargus Jr., W. A., Nakles, M. R., Pote, B., and Tedrake, R., "Effect of Anode Current Fluctuations on Ion Energy Distributions within a 600 W Hall Effect Thruster," *Proceedings of the 44th Joint Propulsion Conference and Exhibit*, No. AIAA-2008-4724, American Institute of Aeronautics and Astronautics, Hartford, CT, July 2008.

[14]Hargus Jr., W. A. and Nakles, M. R., "Ion Velocity Measurements within the Acceleration Channel of a Low Power Hall Thruster," *Proceedings of the 30th International Electric Propulsion Conference*, No. IEPC-2007-172, Florence, Italy, September 2007.

[15]Randolf, T., Kim, V., Kaufman, H., Korzubusky, K., Zhurin, V., and Day, M., "Facility Effects on Stationary Plasma Thruster Testing," *Proceedings of the 23rd International Electric Propulsion Conference*, No. IEPC-93-93, Seattle, WA, September 1993.